DE LA RECHERCHE À L'INDUSTRIE

COPIL BIGMECA – 02/03/3023

Vers l'identification des lois de plasticité cristalline par apprentissage statistique et jumeau numérique

MESBAH Daria[1,2], GELEBART Lionel[1], RYCKELYNCK David[2], PROUDHON Henry[2]

[1] Université Paris-Saclay, CEA, Service de Recherches Métallurgiques Appliquées, 91191 Gif-sur-Yvette

[2] Mines Paris, Université PSL, Centre des Matériaux (MAT), UMR7633 CNRS, 91003 Evry, France

- **Crystal Plasticity (CP) models, accounting for microstructural heterogeneity, allows the investigation of intragranular deformation**

- **Confront crystal plasticity simulations with microscopic observations of deformation**
  - Today, either at **macroscopic** (effective response) or **microscopic** scale but **surface** data
  - Benefit from **3DXRD** to enrich experimental data with **microscopic and volume** data

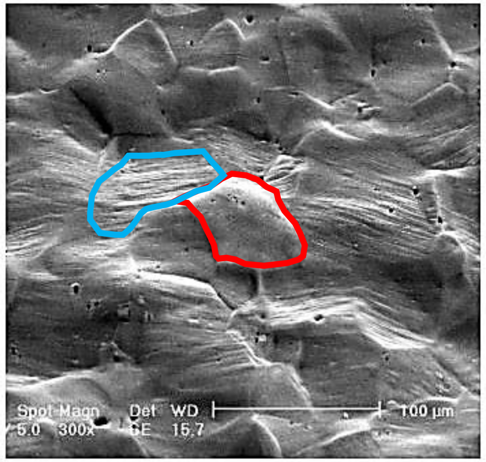

Plane strain stretched Al 6022
(T-Sample at 15% strain)
From Yoon-Suk Choi (PhD thesis)

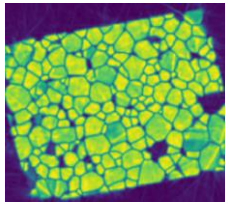

3D X-Ray Diffraction → ***Multiscale confrontation . . .***

Microscopic		***Macroscopic***
Intragranular	*Granular*	*Polycrystal*

. . . towards a multiscale calibration

AMITEX

← ***FFT-based simulations***

← ***Crystal plasticity***

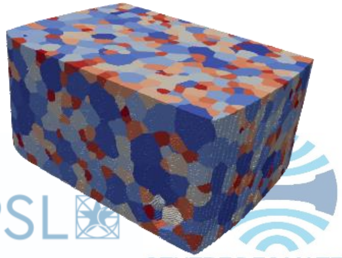

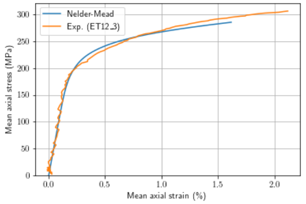

TOWARDS IMAGE-BASED CALIBRATION OF MECHANICAL MODEL

DIFFRACTION-BASED 3D MATERIALS IMAGING

ID11

IN SITU MATERIAL TESTING

Multiscale *experimental data*

$(1 - 10^{-2}\ \mu\text{m})$

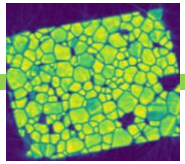

Elastic strain tensor ***maps***

y^{Exp}

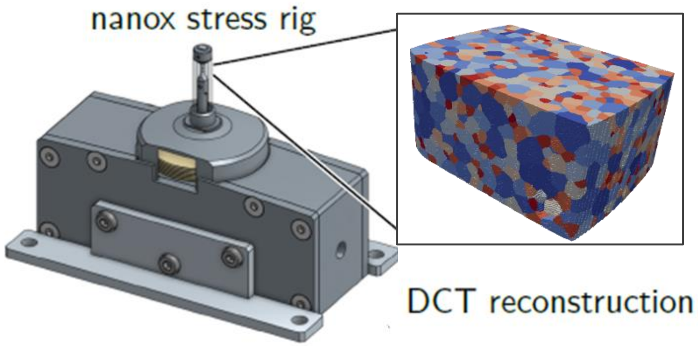

IMAGE-BASED MODEL CALIBRATION

$$\mu_{opt} = \underset{\mu_i}{\operatorname{argmin}} \left\| y^{Simu}(\mu_i) - y^{Exp} \right\|$$

$\boldsymbol{\mu_{i+1}}$

AMITEX

3D images *of microstructure*

MULTISCALE CRYSTAL PLASTICITY FFT (CP-FFT) SIMULATIONS

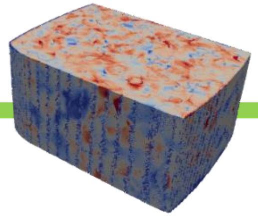

Elastic strain tensor ***maps***

$y^{Simu}(\mu_i)$

CP α-Ti (HCP)

Time-consuming multiscale simulations

Speed-up solutions being investigated:

- *Multi-grid techniques* ➔ ***Zoom Structural***
- *Learning-based methods* ➔ ***Micromechanical super-resolution***

OUTLINE

- CONTEXT AND MOTIVATION
- DIFFRACTION-BASED 3D MATERIALS IMAGING
- CRYSTAL PLASTICITY FFT (CP-FFT) SIMULATIONS
- MICRO-MECHANICAL SUPER-RESOLUTION
- CONCLUSIONS AND OUTLOOKS

- CONTEXT AND MOTIVATION
- DIFFRACTION-BASED 3D MATERIALS IMAGING
- CRYSTAL PLASTICITY FFT (CP-FFT) SIMULATIONS
- MICRO-MECHANICAL SUPER-RESOLUTION
- CONCLUSIONS AND OUTLOOKS

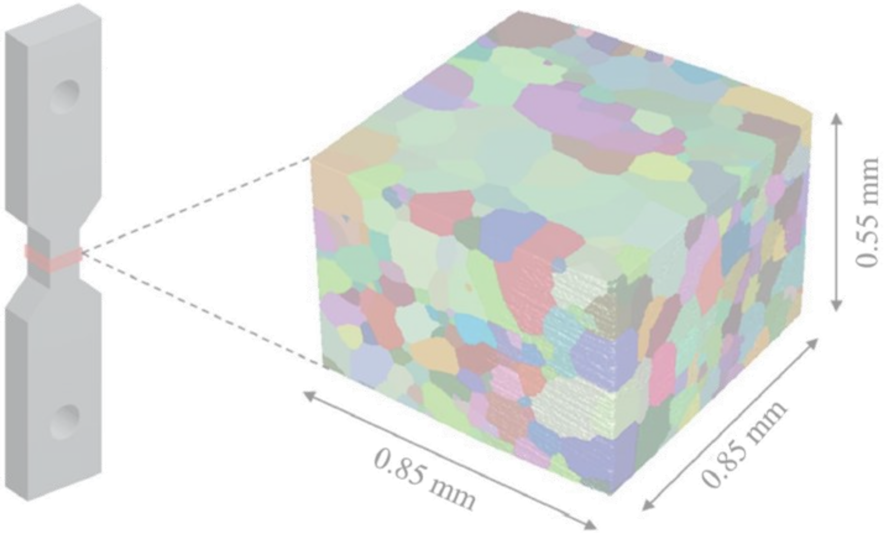

- **Commercially Pure Titanium (α)**

DCT (Near field)

- Undeformed (for CP simulations)
- Deformed (average orientation per grain)
- **Detector resolution**: $r^{DCT} = 1.6\ \mu m$
- Volume $5 \times (650 \times 650 \times 150)\ \mu m^3$
- Raw data: $5 \times 58 = 290\ Go$

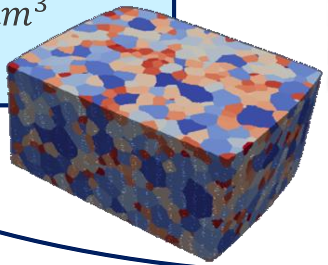

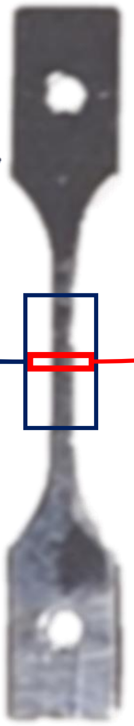

Scanning-3DXRD

- Deformed state
- Spatial resolution:

$$r^{s3DXRD} = 300\ \mathbf{nm}$$

- Strain resolution: 10^{-4}

➔ **Fine maps of elastic strain tensor and desorientation angle**

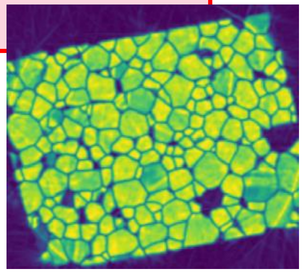

3DXRD (Far field)

- Deformed state
- **Per grain** elastic strain tensor and desorientation angle
- Detector resolution:

$$r^{3DXRD} = 50\ \mu m$$

- **Strain resolution** : 10^{-4}

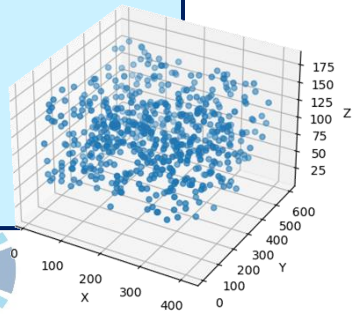

Diffraction figures for different detector position [Oddershede, 2012]

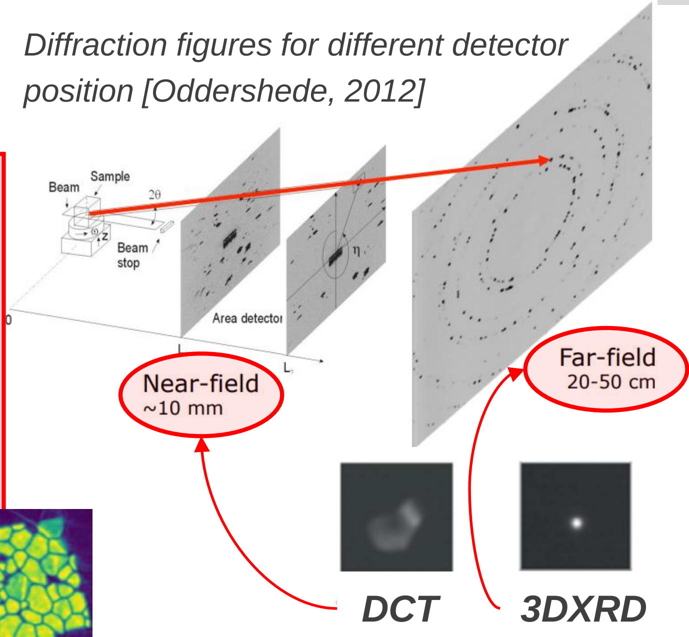

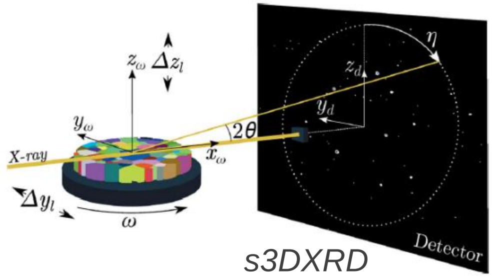

s3DXRD
[Hennigsson, 2020]

Courtesy of C. Ribart (PhD Mines Paris), W. Ludwig, J. Wright (ESRF)

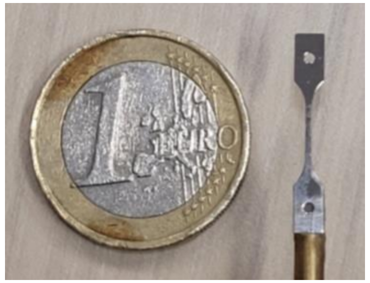

MINES PARIS | PSL

CENTRE DES MATERIAUX P.M FOURT

FABLE 3DXRD

ESRF The European Synchrotron

- CONTEXT AND MOTIVATION
- DIFFRACTION-BASED 3D MATERIALS IMAGING
- CRYSTAL PLASTICITY FFT (CP-FFT) SIMULATIONS
- MICRO-MECHANICAL SUPER-RESOLUTION
- CONCLUSIONS AND OUTLOOKS

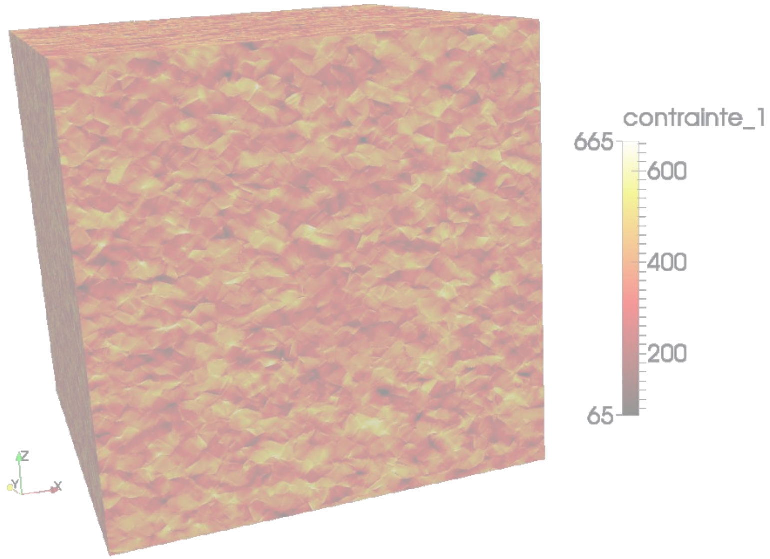

***Large deformation* [Mandel, 1973]**
$F = F^e F^p$

***Polar decomposition* of elastic strain gradient**
$F^e = R^e U^e$

***Crystal Plasticity* (specific to HCP structures)**

Dislocation densities [Alankar et al., 2011]

Phenomenological model [Barkia 2014] (adapted from Méric-Cailletaud model)

Schmid law	$\tau^s = \bar{\bar{\sigma}} : \overline{\overline{m^s}}$
Yield function	$f^s = \lvert\tau^s\rvert - r^s$
Non-linear isotropic hardening	$r^s = \boldsymbol{\tau_C^{F(s)}} + \boldsymbol{Q^{F(s)}} \sum_r h^{rs}\left[1 - \exp\left(-\boldsymbol{b^{F(s)}} v^r\right)\right]$
Hyperbolic viscoplastic flow rule	$\dot{v}^s = \boldsymbol{\dot{v}_0^{F(s)}} \sinh\left\langle \frac{f^s}{\boldsymbol{\sigma_0^{F(s)}}} \right\rangle$
Plastic shear rate	$\dot{\gamma}^s = \dot{v}^s sign(\tau^s)$

Slip systems in HCP Titanium [Battaini, 2017]

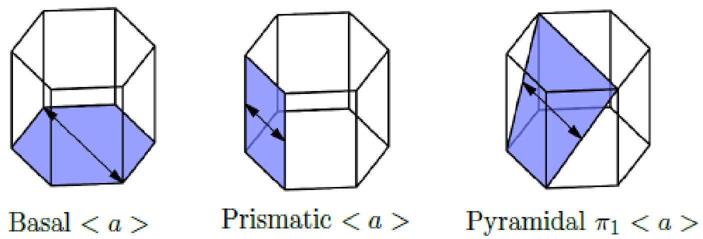

Slip family	Basal	Prism.	Pyr. 1A
$F(s)$	B	P	$\pi_1\langle a\rangle$
Critical Resolved Shear Stress	$\tau_C^{F(s)}$		
Non-linear isotropic hardening	$Q^{F(s)}$, $b^{F(s)}$		
Viscosity	$\dot{v}_0^{F(s)}$, $\sigma_0^{F(s)}$		

MODEL IDENTIFICATION = 15 PARAMETERS TO CALIBRATE

- **Introduced by [Moulinec and Suquet, 1994]**
  - Global and local response of composites with elastic behaviour
- **Specificities:**
  - No meshing required
    - DCT reconstruction as input for simulations
  - Massively parallel implementation
  - Limited to problems with periodic boundary conditions
- **Applications: crystal plasticity, composites, fracture, …**

Initialisation : $\varepsilon^0(x) = E$ et $\sigma^0(x) = C(x) : \varepsilon^0(x) \quad \forall x \in V$

Itération $i+1$: ε^i et σ^i étant supposés connus

1. $\tau^i(x) = \sigma^i(x) - C^0 : \varepsilon^i(x)$
2. $\hat{\tau}^i(x) = \mathscr{F}(\tau^i)$
3. Test de convergence $\boxed{\dfrac{\langle |\xi_j \hat{\sigma}_{ij}| \rangle}{\|\hat{\sigma}(\xi = 0)\|} < \delta}$
4. $\hat{\varepsilon}^{i+1} = -\hat{\Gamma}^0(\xi) : \hat{\tau}^i(\xi)$
5. $\varepsilon^{i+1} = \mathscr{F}^{-1}\left(\hat{\varepsilon}^{i+1}\right)$
6. $\sigma^{i+1}(x) = C(x) : \varepsilon^{i+1}(x)$

AMITEX

Axial strain field

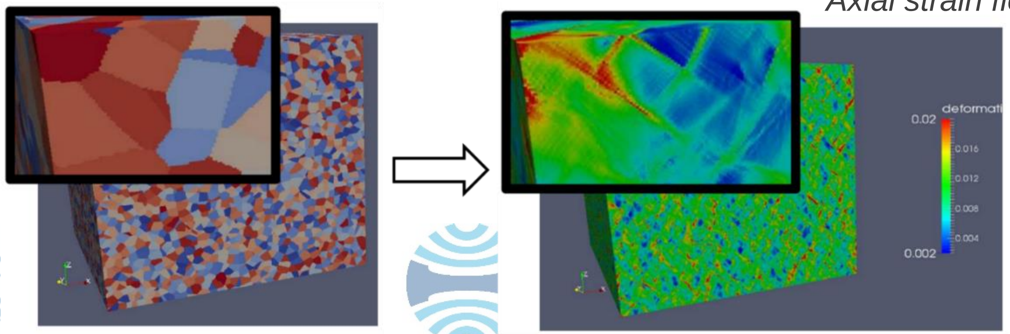

CPFFT simulations:
- *42 875 grains*
- 1024^3 *voxels*
- *4h / 1024 CPU*

[Gélébart et al., 2017]

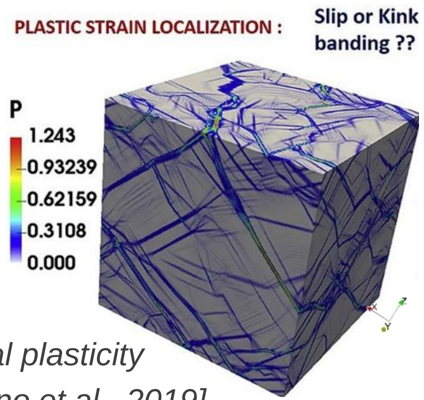

Crystal plasticity [Marano et al., 2019]

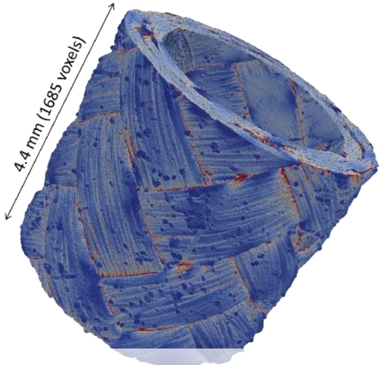

SiC/SiC composites (CT scan) [Chen et al., 2019]

CRYSTAL PLASTICITY FFT (CP-FFT) SIMULATIONS

MACROSCOPIC CALIBRATION OF CRYSTAL PLASTICITY MODEL

- **Identify microstructural parameters leading to a RVE in terms of macroscopic response**
- **Among investigated parameters :**
  1. Number of grains per direction N (N^3 grains in volume)
  2. Resolution per grain per direction r (r^3 voxels in average per grain)
  3. Microstructure type (Arlequin / cubic or Voronoï)

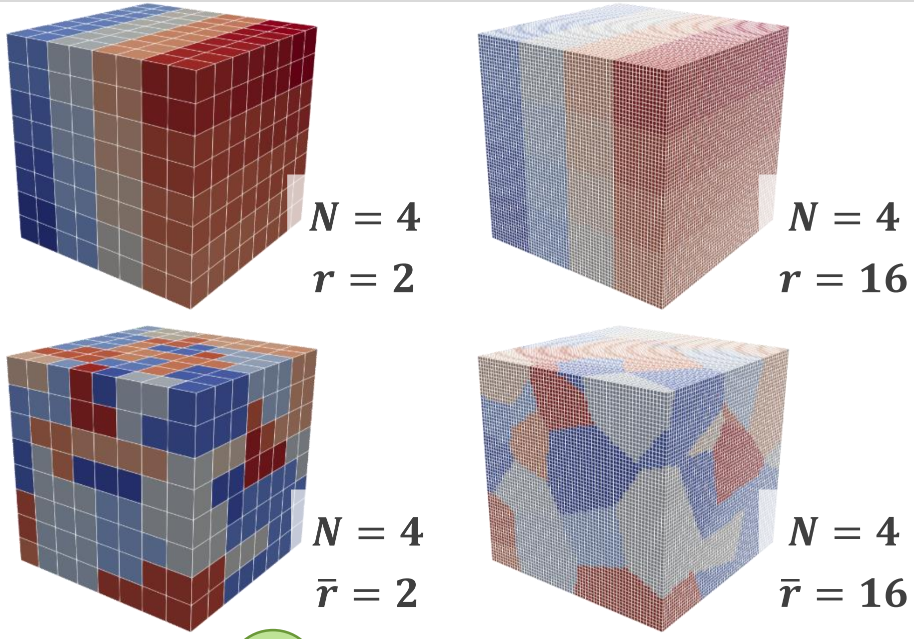

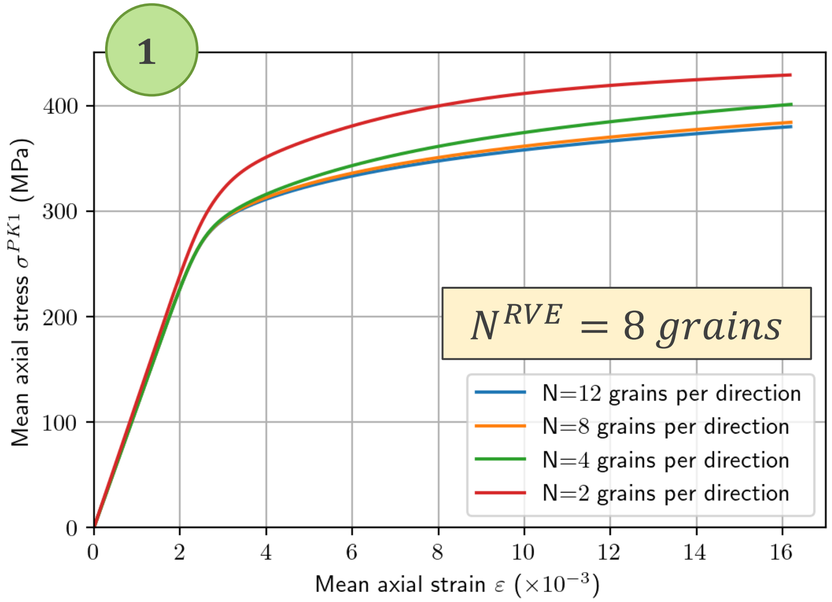

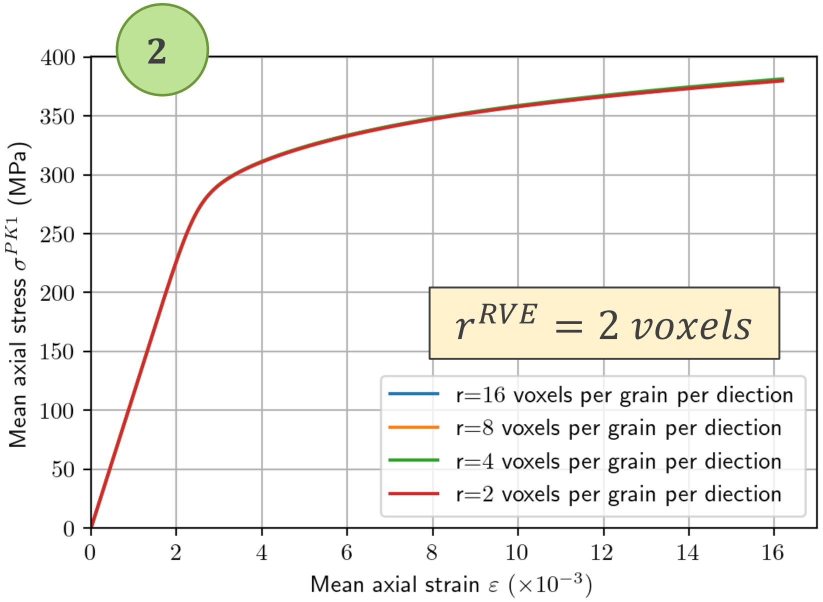

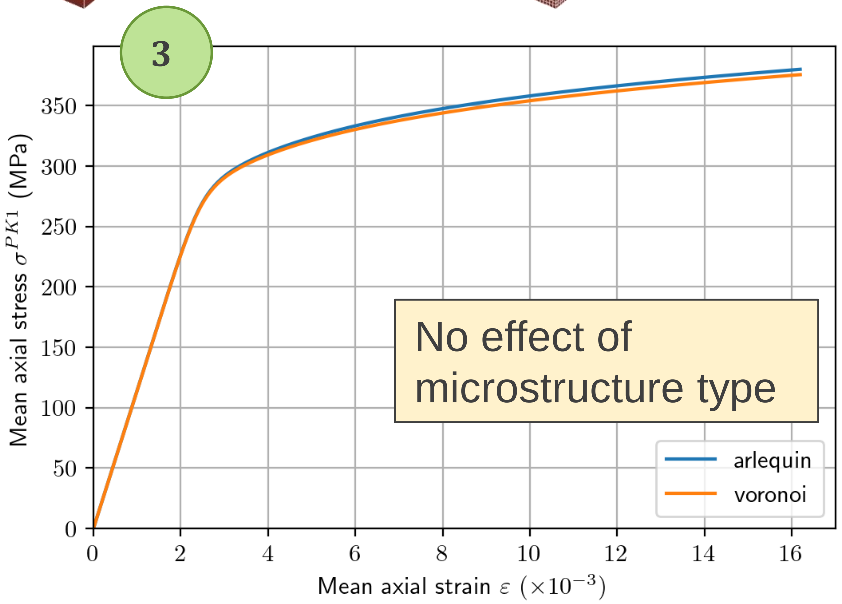

- **RVE parameters assessed in previous study:**
  - $N^{RVE} = 8$ grains per direction
  - $r^{RVE} = 2$ voxels per grain per direction

$\boldsymbol{V = (Nr)^3 = 4096}$ **voxels in volume**

- **Tensile test performed on Ti sample (RD)**

- **Mean field calibration**
  - Mean-squared error as error metric
  - Nelder-Mead optimization function
  - 150 iterations required

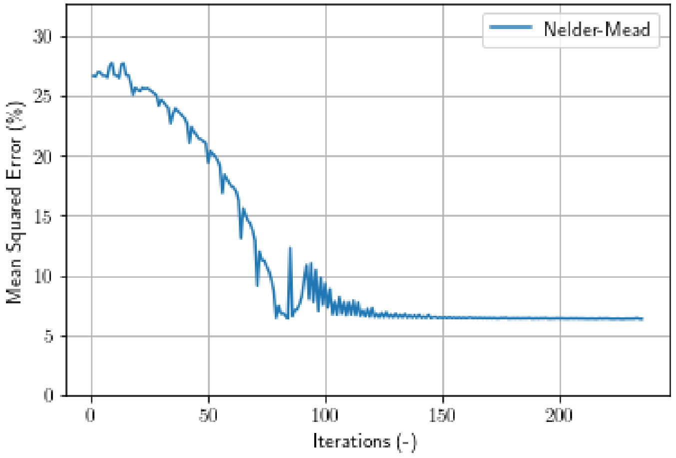

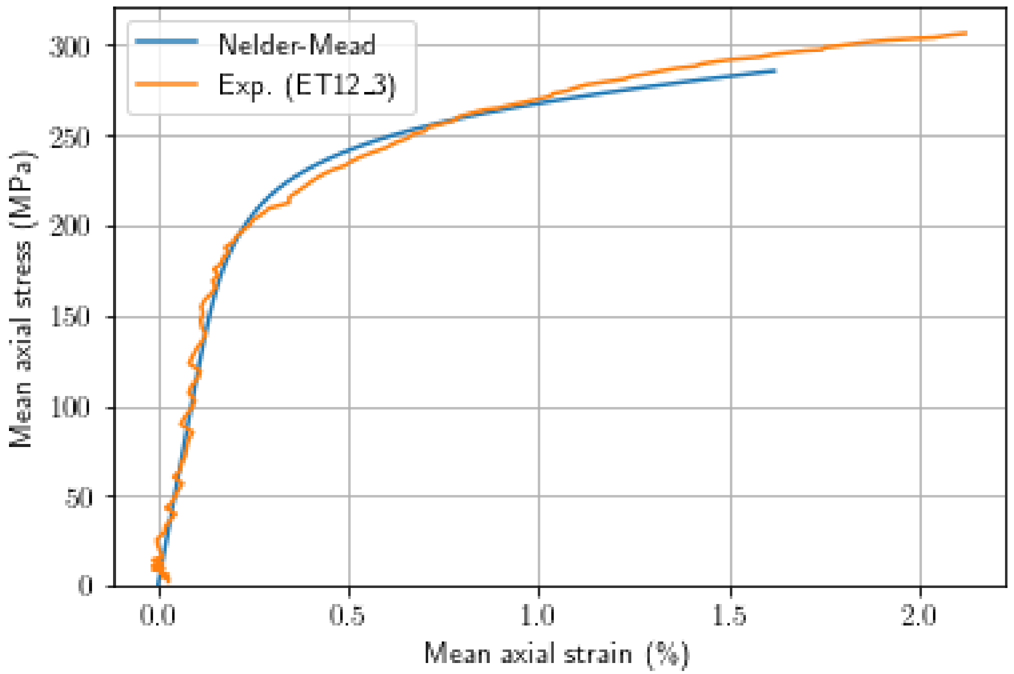

Calibration of **15 crystal plasticity** parameters using a **unique macroscopic response**

OUTLINE

- CONTEXT AND MOTIVATION
- 3D MATERIALS CHARACTERIZATION
- CRYSTAL PLASTICITY FFT (CP-FFT) SIMULATIONS
- **MICRO-MECHANICAL SUPER-RESOLUTION**
- CONCLUSIONS AND OUTLOOKS

“ Single image super-resolution is a **notoriously challenging ill-posed problem** that aims to obtain a HR output from one of its LR versions. ”
[Yang et al., 2019]

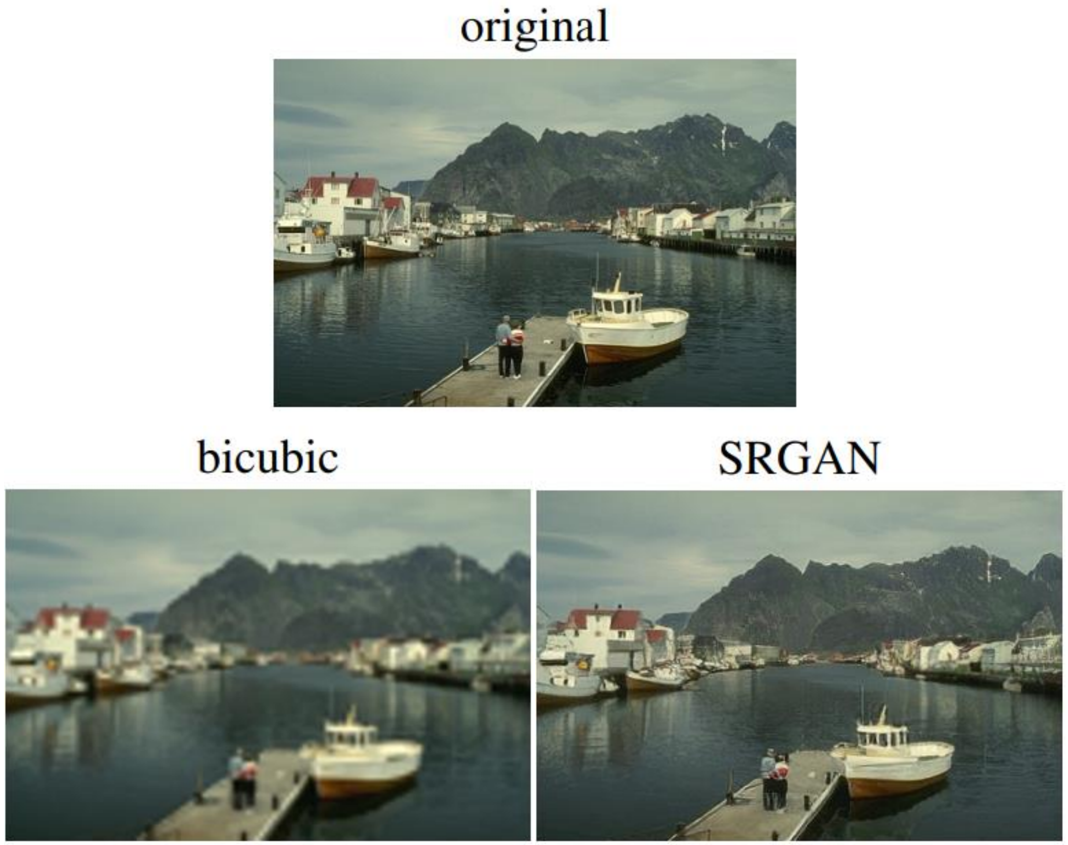

AUTOENCODERS FOR LEARNING-BASED SUPER-RESOLUTION

Animation - SRCNN [Dong et al., 2014]

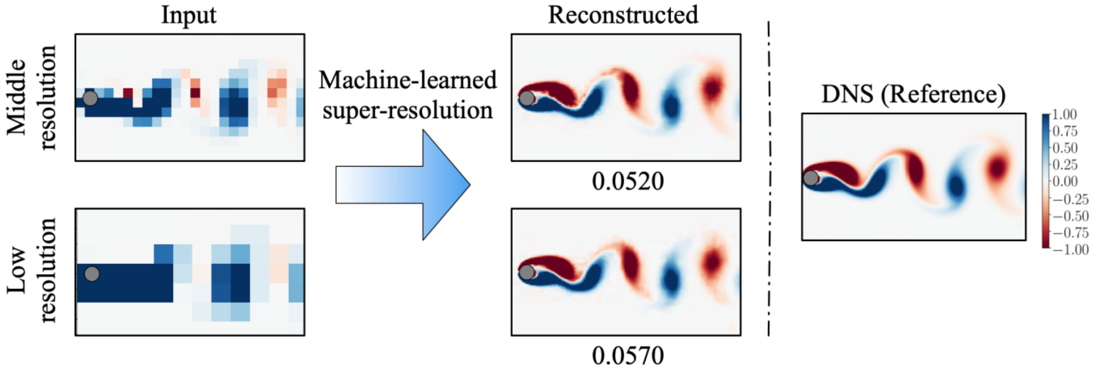

Fluid mechanics [Fukami et al., 2019]

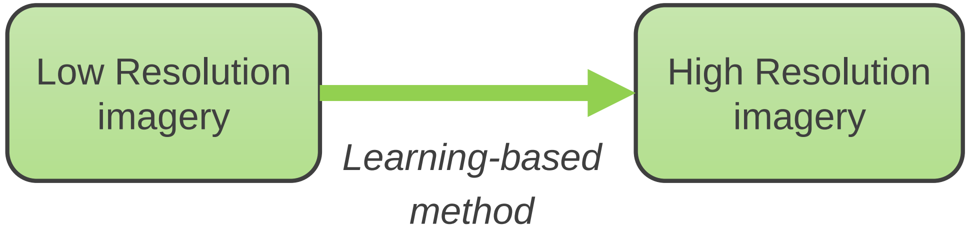

Knee MRI images [Trinh et al., 2014]

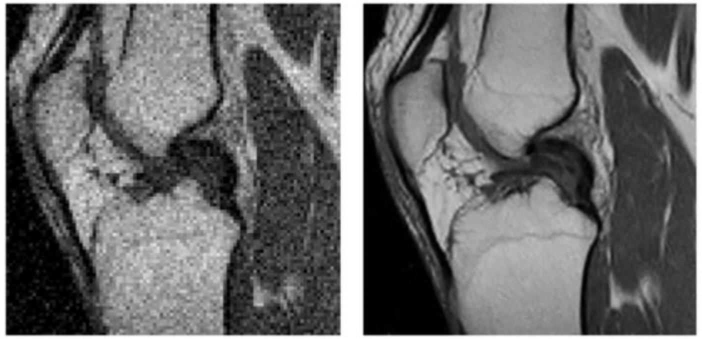

Biphased microstructure [Jung et al., 2021]

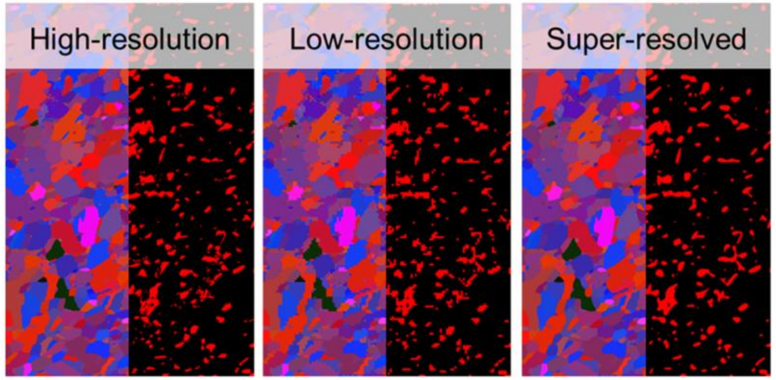

Stress field predictions - PhySRNet [Arora, 2022]

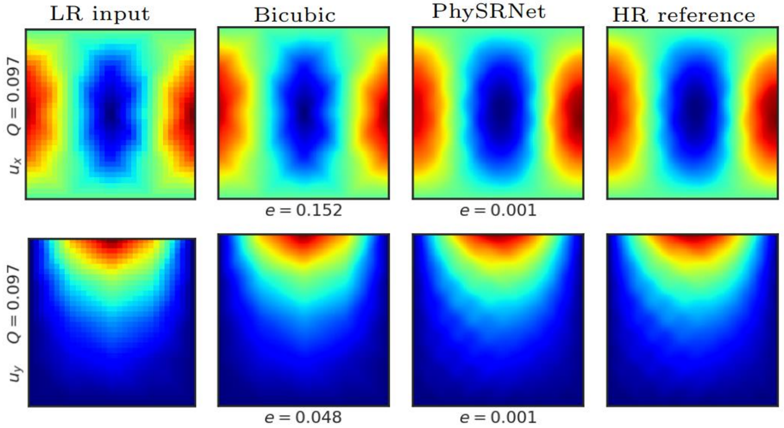

- **Learning-based Super-Resolution applied to different representations of microstructures**
    - **Orientations relationship** (Schmid factor) ➔ **Discrete**
    - **Morphology relationship** (Distance to closest grain boundaries) ➔ **Continuous**
    - **Stress state** (Stress tensor components for a tensile simulation) ➔ **Piecewise**

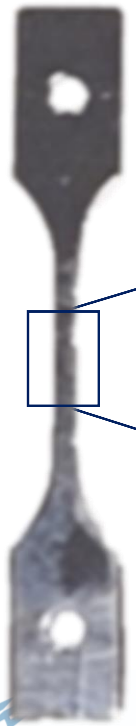

DCT scan

1853 grains

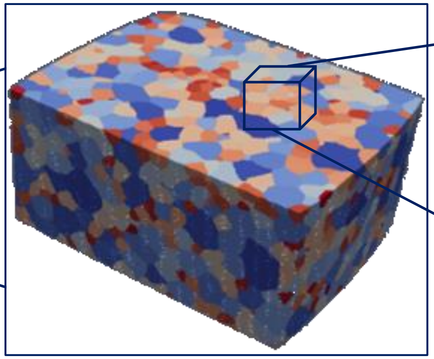

$276 \times 532 \times 652\ \mu m^3$

$127 \times 245 \times 300\ voxels$

Submodels extraction

4×10^3 instances

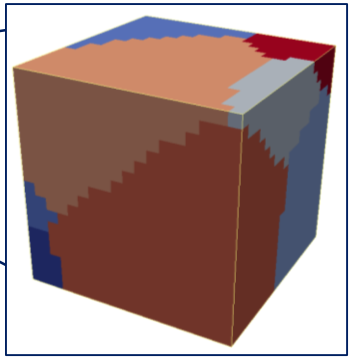

$70^3\ \mu m^3$

$32^3\ voxels$

Data augmentation for training (1000 submodels)

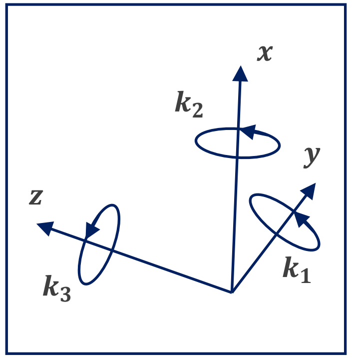

10 random combination $[\![k_1, k_2, k_3]\!]$ of 90° rotations around x, y and z axes

$10^3 \rightarrow 10^4$ ***training data***

Orientations field

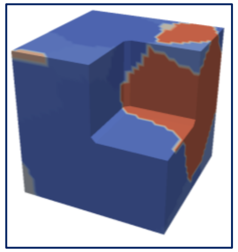

Morphologies field

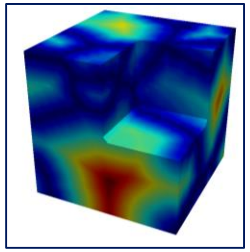

Stress field

Work in Progress

MINES PARIS | PSL

CENTRE DES MATERIAUX P.M FOURT

CONVOLUTIONAL NEURAL NETWORK FOR SUPER-RESOLUTION

Input $(32^3 \times c)$	4* Conv3D + BatchNorm	Flatten + **Latent** $(512 \times c)$+ Dense + Reshape	4 * Conv3D_Transpose	**Output** $(32^3 \times c)$

Orientations field

Original HR (32, 32, 32) | Original LR ($f = 2$) (32, 32, 32) | SRCNN3D

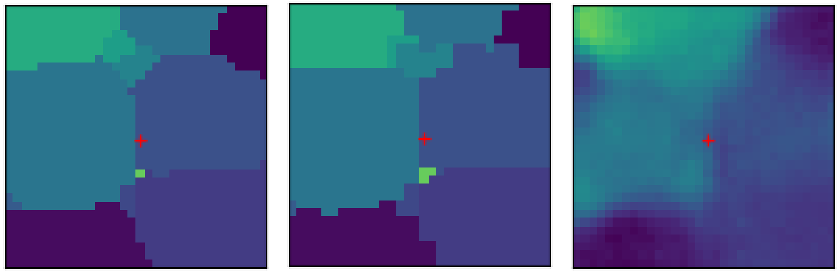

Error: $\frac{||y^{real} - y^{pred}||}{||y^{real}||}$

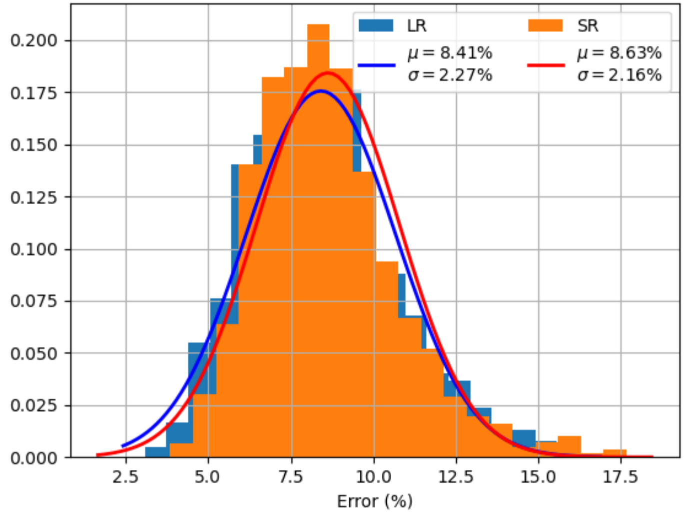

Morphologies field

Original HR (32, 32, 32) | Original LR ($f = 2$) (32, 32, 32) | SRCNN3D

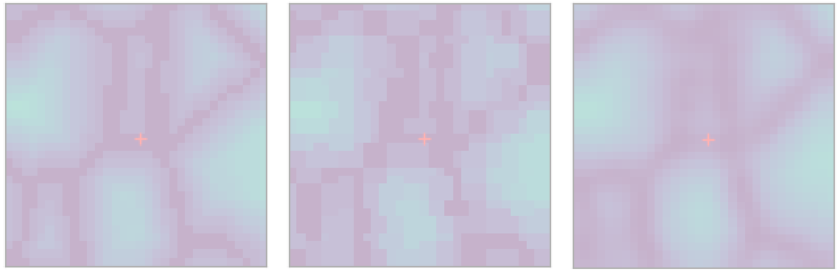

Error: $\frac{||y^{HR} - y^{i}||}{||y^{HR}||}$

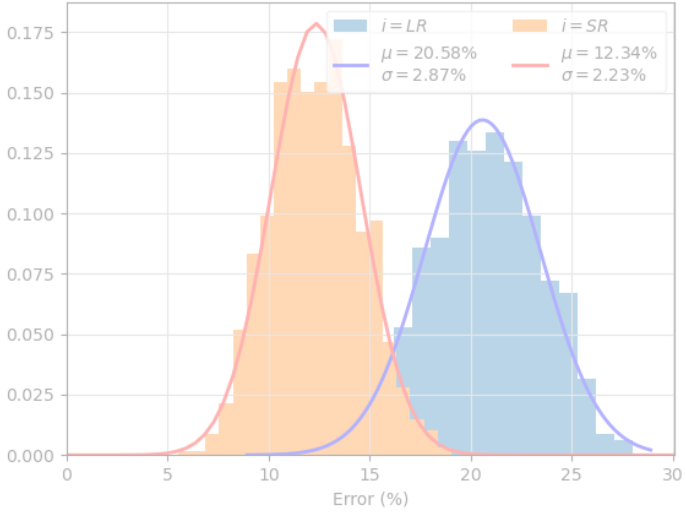

Stress field

Original HR (32,32,32) | Original LR (f=2) (32,32,32) | SRCNN3D

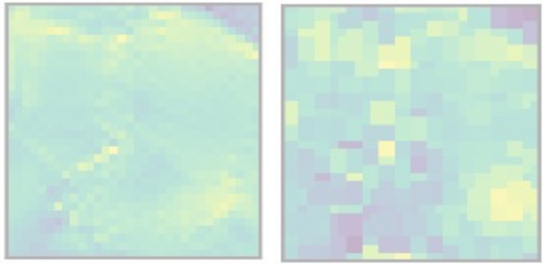

Work in Progress . . .

CONVOLUTIONAL NEURAL NETWORK FOR SUPER-RESOLUTION

Input $(32^3 \times c)$	4* Conv3D + BatchNorm	Flatten + **Latent** $(512 \times c)$+ Dense + Reshape	4 * Conv3D_Transpose	Output $(32^3 \times c)$

Orientations field

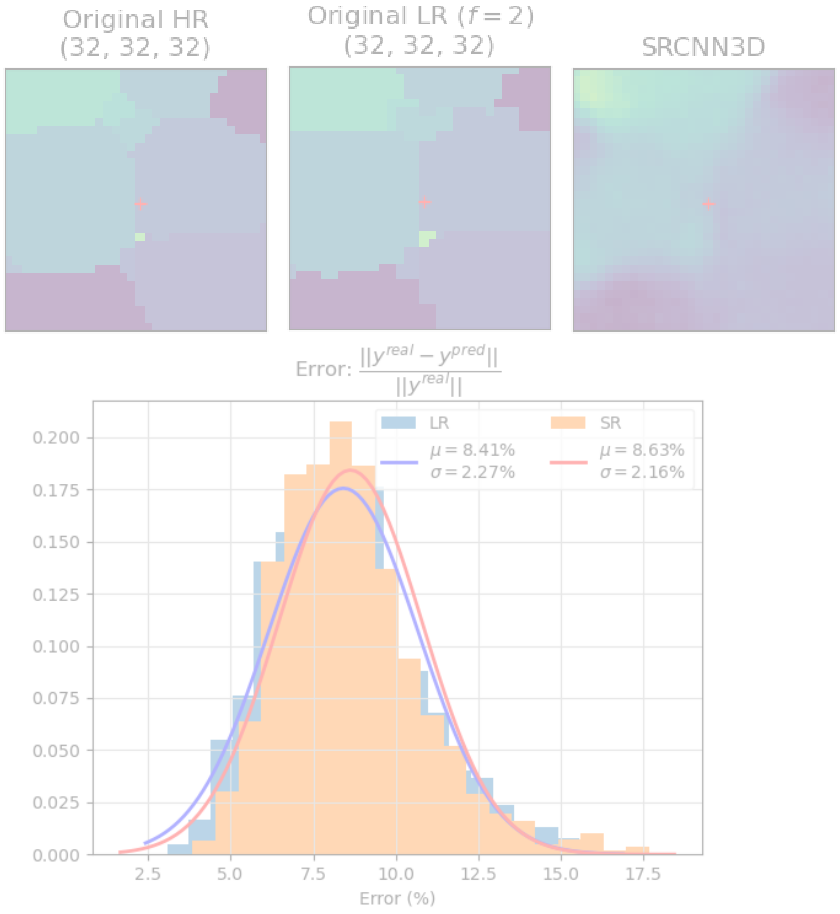

Morphologies field

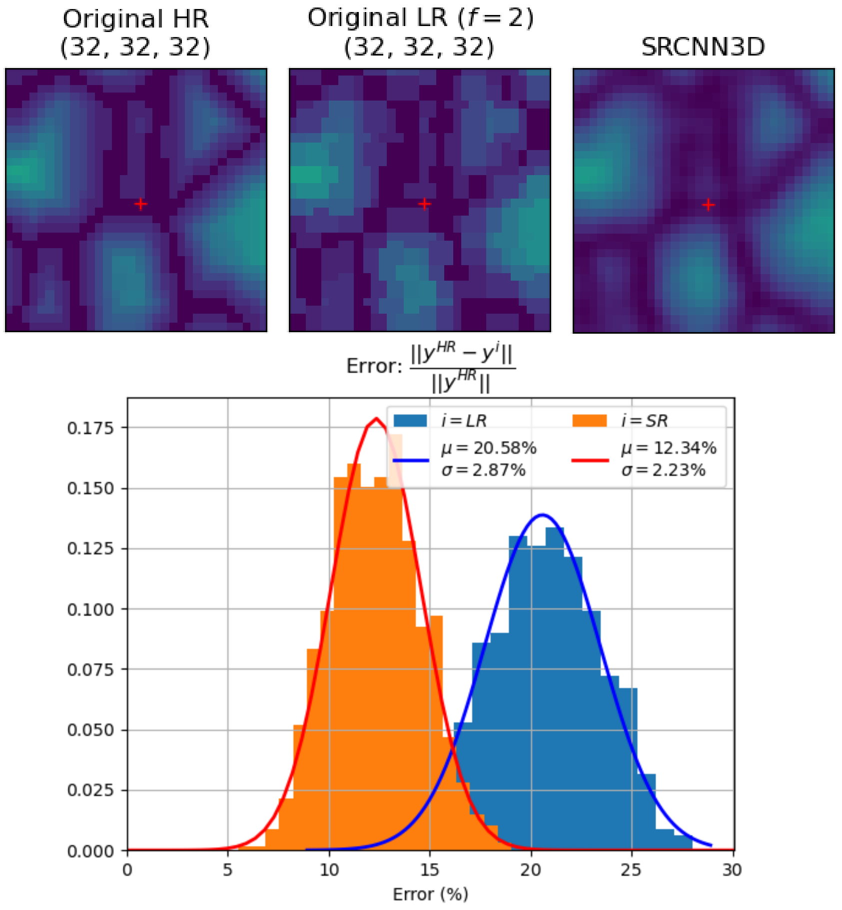

Stress field

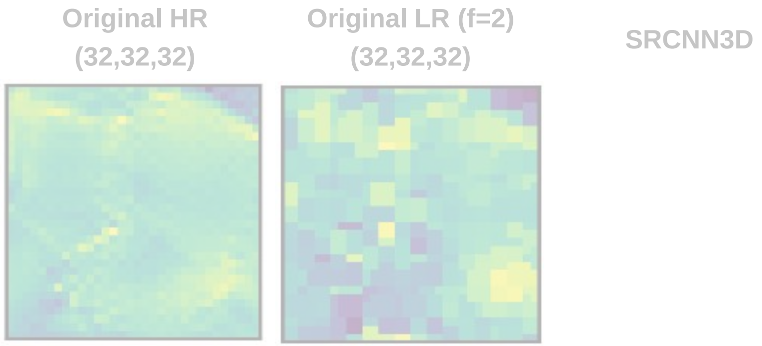

Work in Progress . . .

MICRO-MECHANICAL SUPER-RESOLUTION

CONVOLUTIONAL NEURAL NETWORK FOR SUPER-RESOLUTION

Input $(32^3 \times c)$	4* Conv3D + BatchNorm	Flatten + **Latent** $(512 \times c)$+ Dense + Reshape	4 * Conv3D_Transpose	**Output** $(32^3 \times c)$

Orientations field

Original HR (32, 32, 32) | Original LR ($f=2$) (32, 32, 32) | SRCNN3D

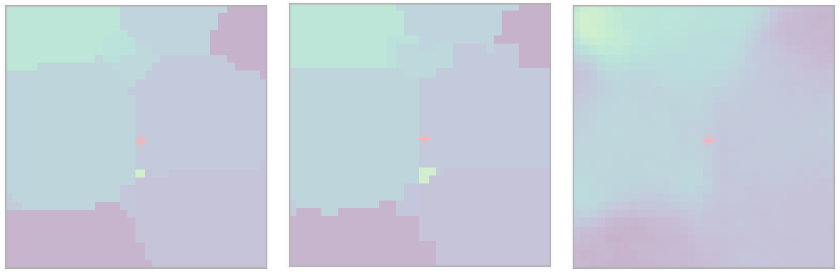

Error: $\frac{||y^{real} - y^{pred}||}{||y^{real}||}$

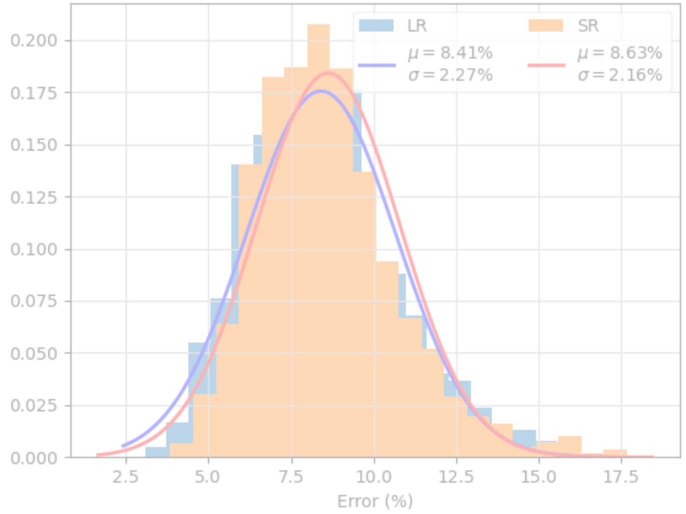

Morphologies field

Original HR (32, 32, 32) | Original LR ($f=2$) (32, 32, 32) | SRCNN3D

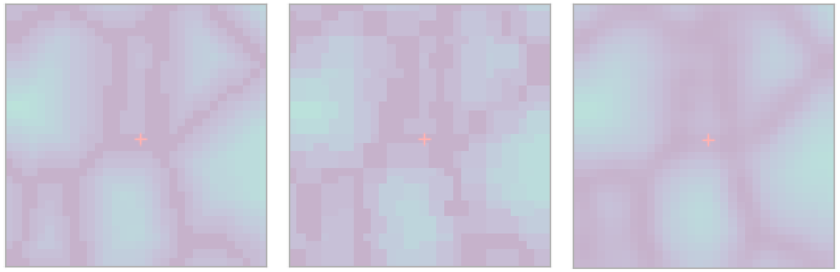

Error: $\frac{||y^{HR} - y^{i}||}{||y^{HR}||}$

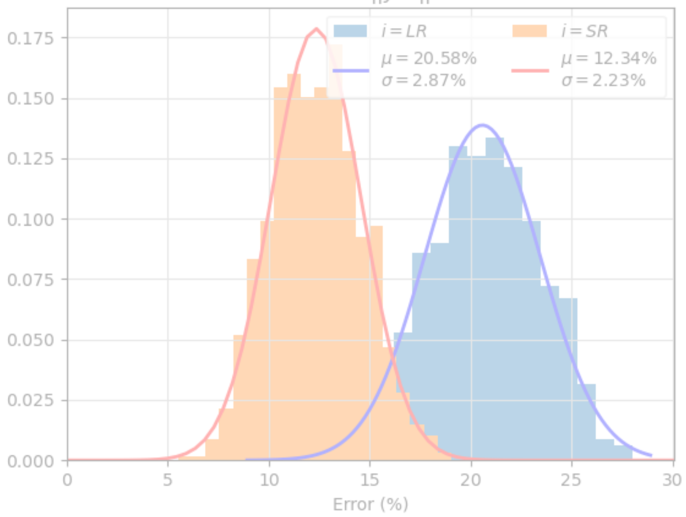

Stress field

Original HR (32,32,32) | **Original LR (f=2) (32,32,32)** | **SRCNN3D**

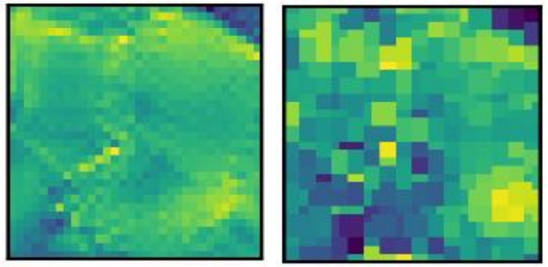

Work in Progress . . .

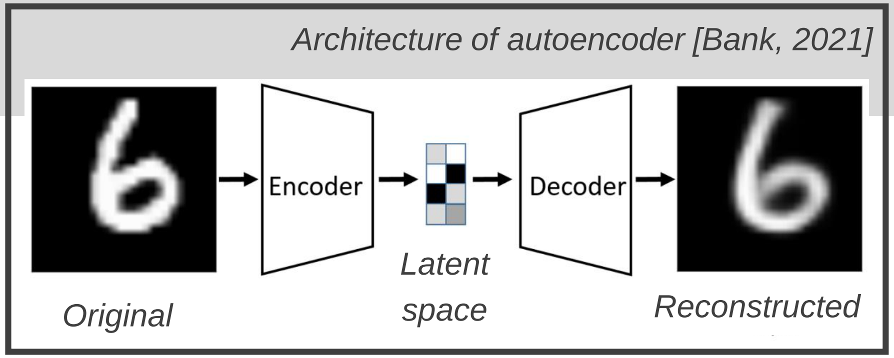

- **Multimodality**
  - Benefit from correlations between multiple representations (MCOVID-Net for COVID diagnosis)
  - Perform cross modal reconstruction

- **Applications to welding defects *[Launay et al., 2021]***
  1. **Offline 1:** Learning morphological and mechanical representations of welding defects (**AutoEncoder)**
  2. **Offline 2:** Learning transition between latent representations of each modality **(Fully-Connected)**.
  3. **Online: For a new defect with a given morphology,** reconstruct the induced mechanical field distortions.

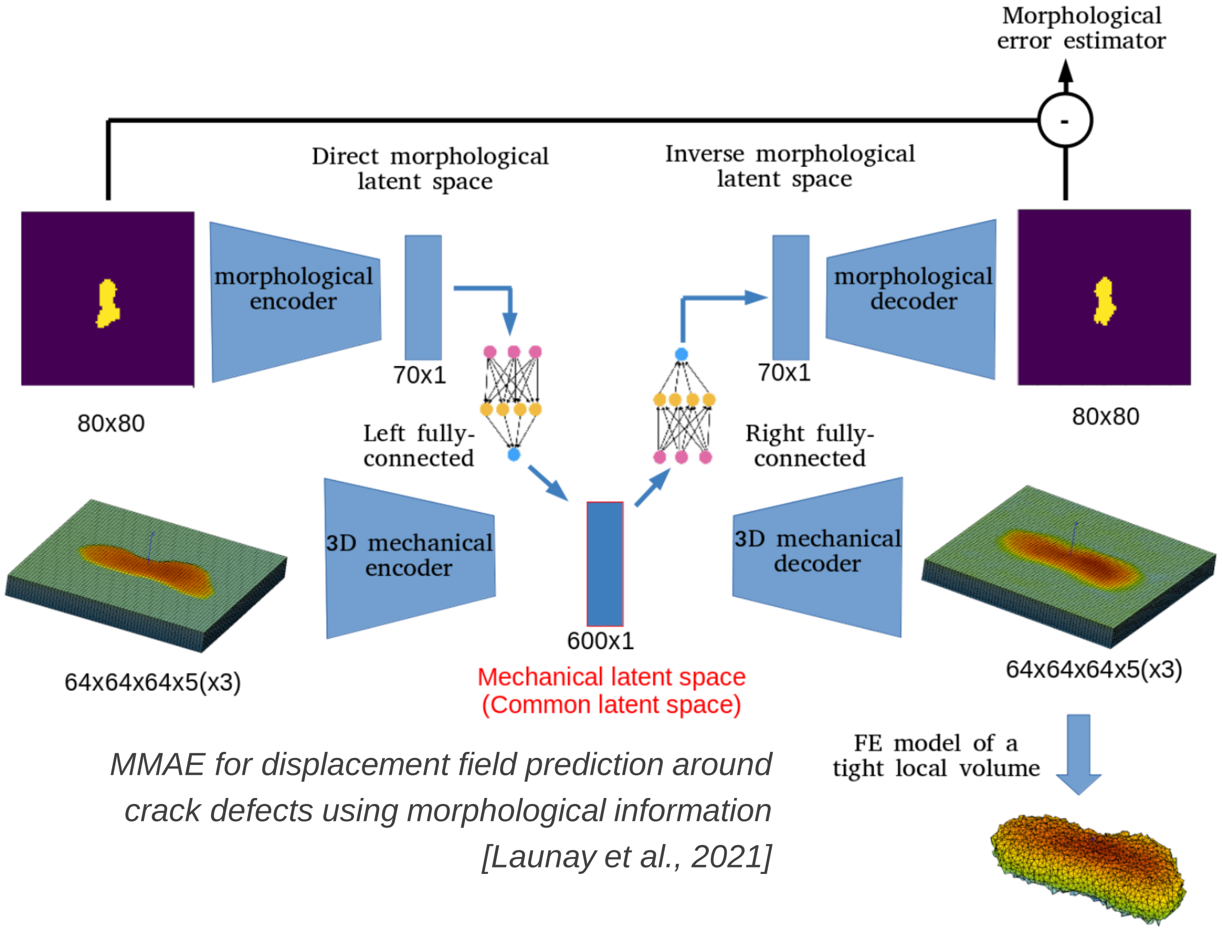

MMAE for displacement field prediction around crack defects using morphological information [Launay et al., 2021]

APPLICATION OF MULTIMODAL AUTOENCODER TO MICROMECHANICAL SUPER-RESOLUTION

High Resolution grains morphology

Distance to grain boundaries: (N, 32, 32, 32, 1)

High Resolution grains orientation

Max Schmid factors per slip family: (N, 32, 32, 32, 3)

Low Resolution stress field

10 FFT simulations run with different sets of μ_i
Grossely discretized version of submodels (~2/4 times)
Gross stress representation: (10*N, 32, 32, 32, 9)

High Resolution stress field

10 FFT simulations run with different sets of μ_i
Finely discretized version of submodels.
Fine stress representation: (10*N, 32, 32, 32, 9)

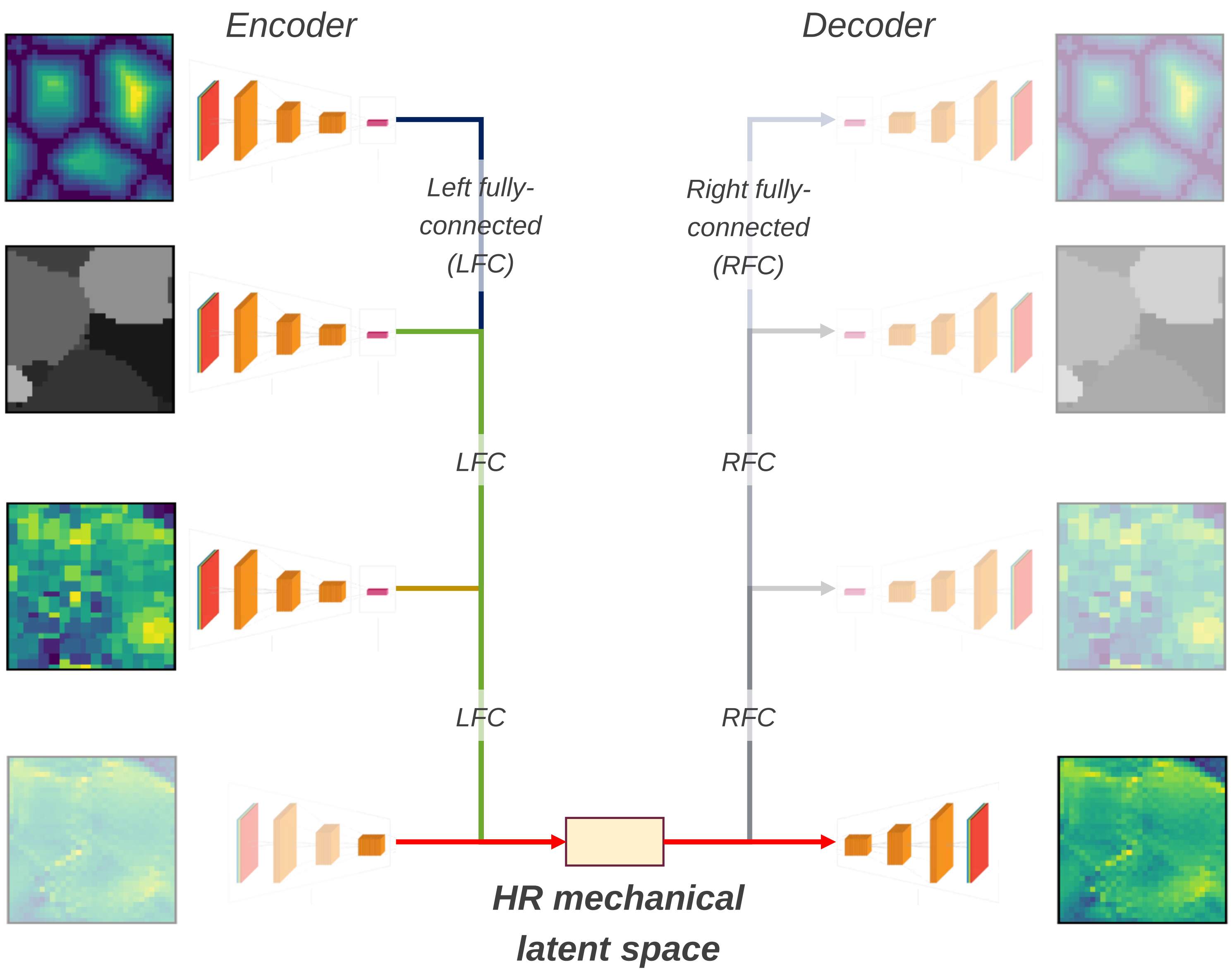

- **Learning / Training phase of MMAE:**
  - Orientations representation → OK
    - « *Maximum Schmid factors per slip family* »
  - Morphological representation: → OK
    - « *Distance to grain boundaries* »
  - Mechanical relationships → WIP

	Schmid Basal	***Schmid Prismatic***	***Schmid Pyr. 1A***	***Distance***
Original (32^3)	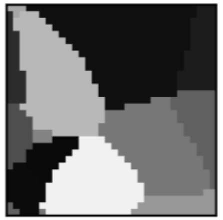	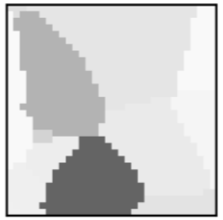	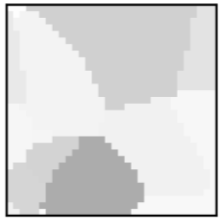	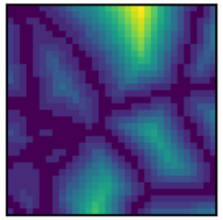
CAE3D (512)	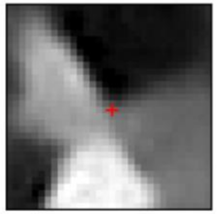	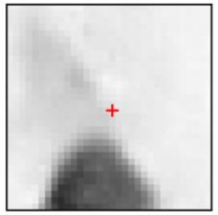	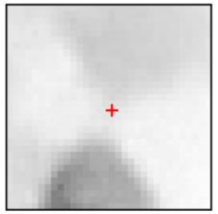	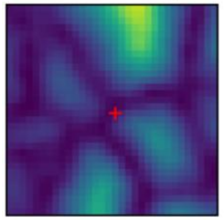

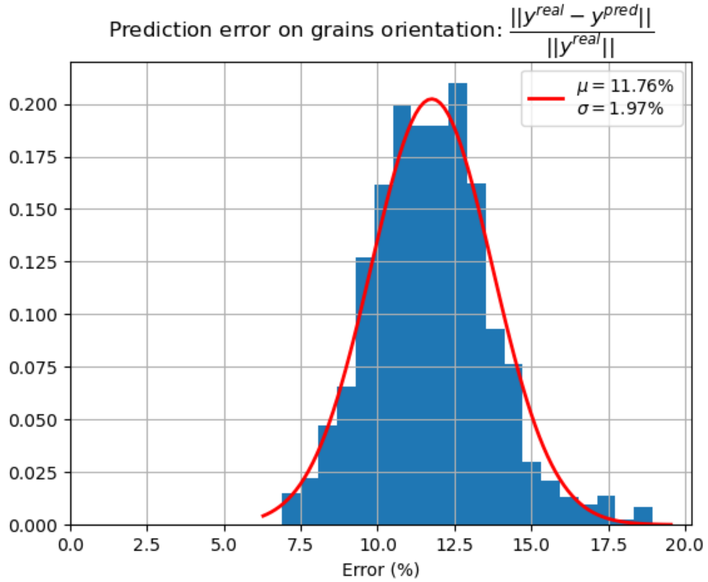

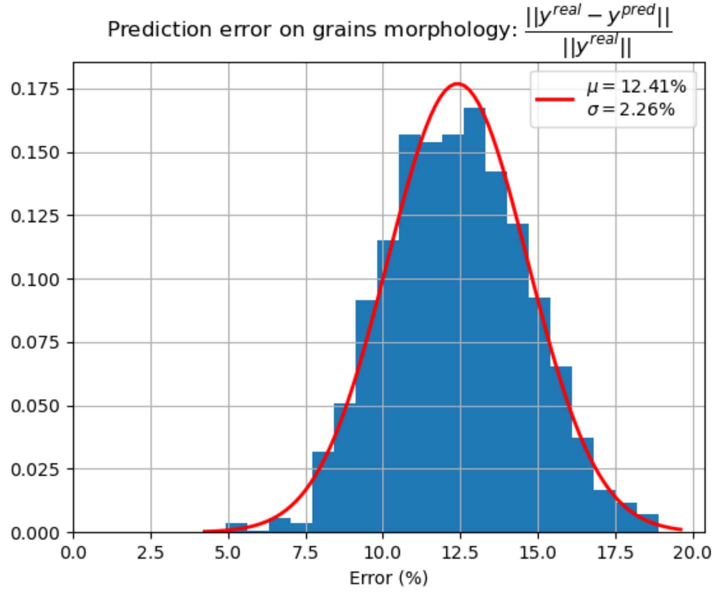

OUTLINE

- CONTEXT AND MOTIVATION
- 3D MATERIALS CHARACTERIZATION
- CRYSTAL PLASTICITY FFT (CP-FFT) SIMULATIONS
- *COMPUTER VISION* FOR IMAGE SUPER-RESOLUTION
- CONCLUSIONS AND OUTLOOKS

Multimodal data acquisition
ESRF – ID11 (09/2022)

Desorientation / Elastic strain field as **QoI** for parameter calibration

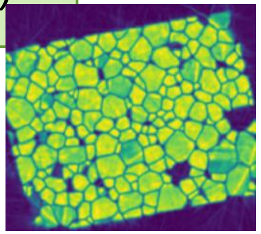

CP model calibration using macroscopic response

RVE parameterization:

- $N = 8$ grains per direction
- $r = 4$ voxels per grain per direction

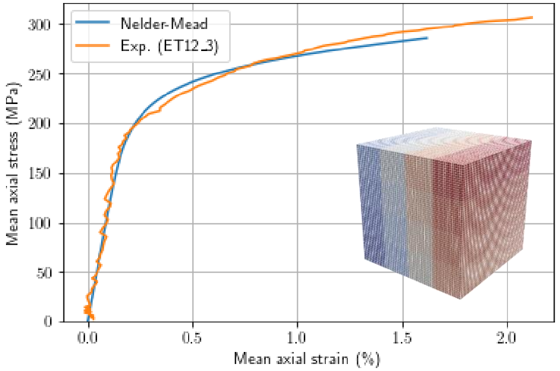

Super-Resolution on microstructure-related information

Schmid factors (orientations)
Distance to grain boundaries

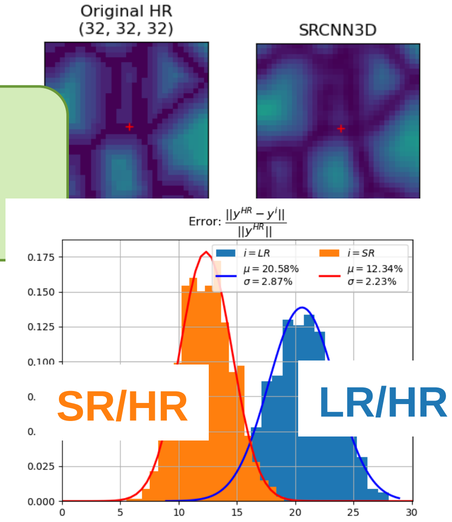

Error

AutoEncoder to learn microstructural attributes

Schmid factors (orientations)
Distance to grain boundaries

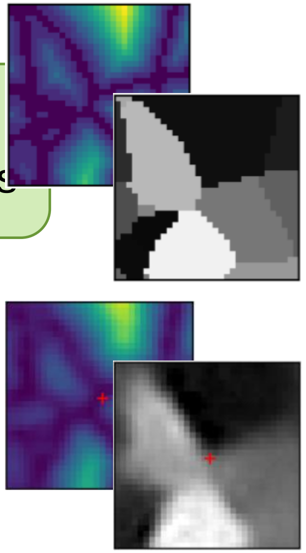

PERSPECTIVES: GRAINS BOUNDARIES (GBs) POSITION

- **During DCT data reconstruction, GBs position obtained through <u>grains dilation</u> (neutral position)**
  - High confidence in grains interior
  - Low confidence in GB neighbourhood
- **Exploration of morphological space using mesh morphing of GBs:**
  - *Random magnitude* of *Laplacian Eigenmodes*
- **Aim: Assess the impact of this uncertainty on the material parameters calibration**

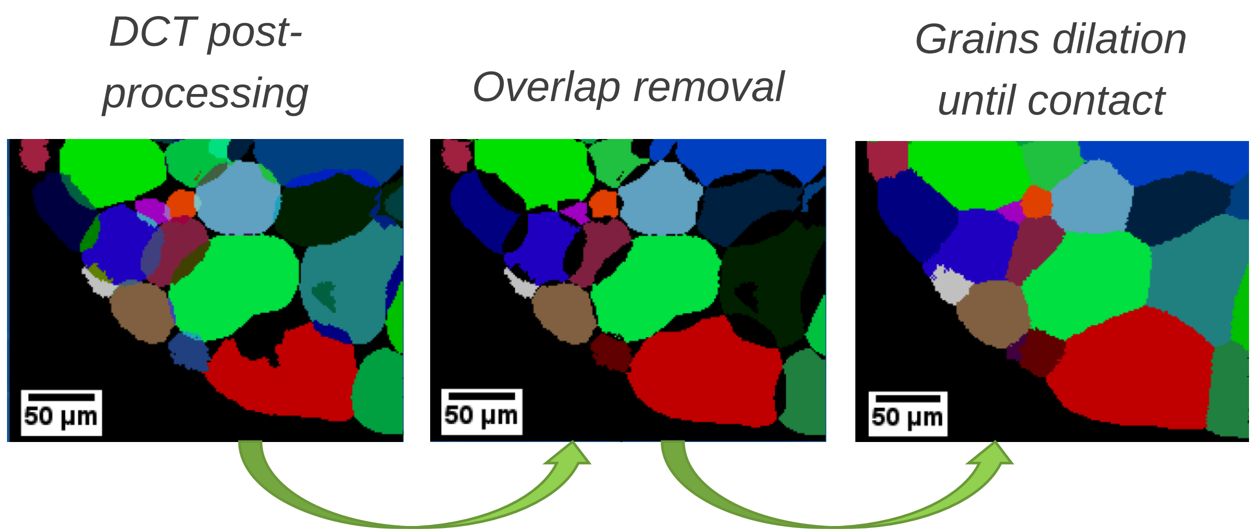

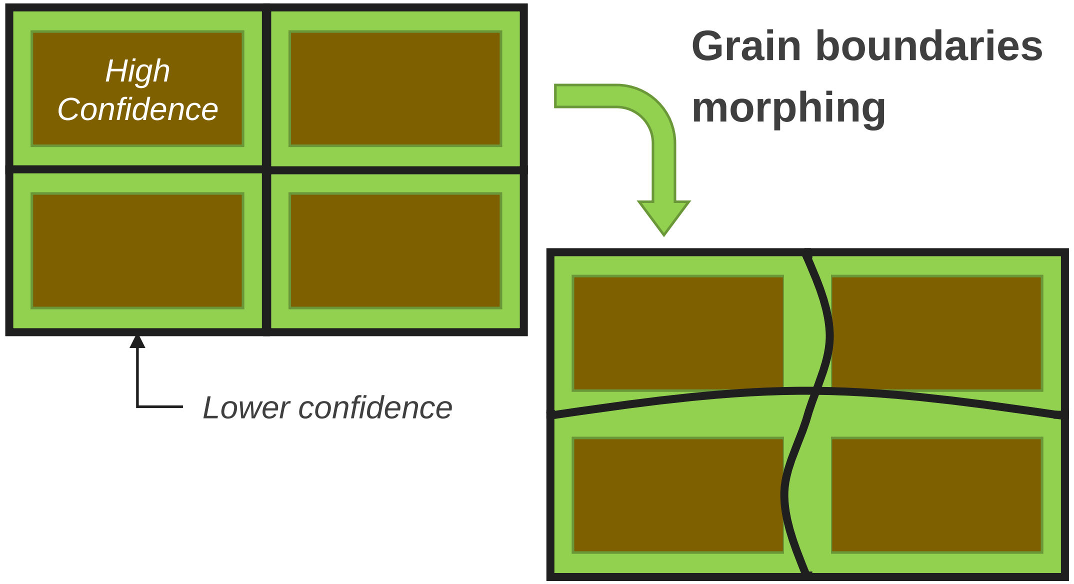

REFERENCES

[Alankar et al., 2011] Alankar, A., Eisenlohr, P., and Raabe, D. (2011). A dislocation density-based crystal plasticity constitutive model for prismatic slip in alpha-titanium. Acta Materialia, 59(18) :7003–7009.

[Arora, 2022] Arora, R. (2022). PhySRNet : Physics informed super-resolution network for application in computational solid mechanics. arXiv :2206.15457 [cond-mat].

[Bank et al., 2021] Bank, D., Koenigstein, N., and Giryes, R. (2021). Autoencoders. arXiv :2003.05991 [cs, stat]

[Barkia, 2014] Barkia, B. (2014). Viscoplasticité à l'ambiante du titane en relation avec ses teneurs en oxygène et hydrogène. PhD thesis, Ecole Polytechnique, Palaiseau, France.

[Battaini, 2017] Battaini, M. (2008). Deformation Behaviour and Twinning Mechanisms of Commercially Pure Titanium Alloys. PhD thesis, Monash University.

[Chen et al., 2019] Analysis of the damage initiation in a SiC/SiC composite tube from a direct comparison between large-scale numerical simulation and synchrotron X-ray micro-computed tomography, International Journal of Solids and Structures, Y. Chen, L. Gélébart, C. Chateau, M. Bornert, C. Sauder, A. King, Volume 161, 2019, Pages 111-126, ISSN 0020-7683, https://doi.org/10.1016/j.ijsolstr.2018.11.009.

[Dong et al., 2014] Dong, C., Loy, C. C., He, K., and Tang, X. (2015). Image Super-Resolution Using Deep Convolutional Networks. arXiv :1501.00092 [cs].

[Fukami et al., 2019] Fukami, K., Fukagata, K., & Taira, K. (2019). Super-resolution reconstruction of turbulent flows with machine learning. Journal of Fluid Mechanics, 870, 106-120. doi:10.1017/jfm.2019.238

REFERENCES

[Gélébart and Derouillat, 2017] L. Gélébart, J. Derouillat. AMITEX_FFTP - Simulations FFT massivement parallèles en mécanique des matériaux hétérogènes. 13e colloque national en calcul des structures, Université Paris-Saclay, May 2017, Giens, Var, France. hal-01923683

[Henningsson, 2020] Reconstructing intragranular strain fields in polycrystalline materials from scanning 3DXRD data,

[Jung et al., 2021] Jung, J., Na, J., Park, H. K., Park, J. M., Kim, G., Lee, S., and Kim, H. S. (2021). Super-resolving material microstructure image via deep learning for microstructure characterization and mechanical behavior analysis. npj Computational Materials, 7(1) :96.

[Launay et al., 2021] Launay, H., Ryckelynck, D., Lacourt, L., Besson, J., Mondon, A., and Willot, F. (2022). Deep multimodal autoencoder for crack criticality assessment. International Journal for Numerical Methods in Engineering, 123(6) :1456–1480.

[Moulinec and Suquet, 1994] A fast numerical method for computing the linear and nonlinear mechanical properties of composites. H. Moulinec, P. Suquet. Comptes Rendus de l'Académie des sciences. Série II. Mécanique, physique, chimie, astronomie, Gauthier-Villars, 1994. ffhal-03019226f

[Marano et al., 2019] Marano, A. (2019). Numerical simulation of strain localization in irradiated polycristals. PhD thesis, Ecole Nationale Supérieure des Mines de Paris.

[Trinh et al., 2014] Trinh, D.-H., Luong, M., Dibos, F., Rocchisani, J.-M., Pham, C.-D., Nguyen, T.Q. Novel example-based method for super-resolution and denoising of medical images (2014) IEEE Transactions on Image Processing, 23 (4), art. no. 6748079, pp. 1882-1895.

THANK YOU FOR YOUR ATTENTION

- **Contact:**
  - daria.mesbah@cea.fr
  - daria.mesbah@mines-paristech.fr